Available online at www.sciencedirect.com
ScienceDirect
Journal of Hazardous Materials 153 (2008) 261–268
Journal of Hazardous Materials
www.elsevier.com/locate/jhazmat

Preparation, characterization, non-isothermal reaction kinetics, thermodynamic properties, and safety performances of high nitrogen compound: Hydrazine 3-nitro-1,2, 4-triazol-5-one complex

Jian-hua Yi, Feng-qi Zhao *, Hong-xu Gao, Si-yu Xu, Min-chang Wang, Rong-zu Hu

Xi'an Modern Chemistry Research Institute, Xi'an 710065, PR China

Received 8 May 2007; received in revised form 20 August 2007; accepted 20 August 2007
Available online 30 August 2007

Abstract

A new high nitrogen compound hydrazine 3-nitro-1,2,4-triazol-5-one complex (HNTO) was prepared by the reaction of 3-nitro-1,2,4-triazol-5-one with hydrazine hydrate, and its structure was characterized by means of organic elemental analyzer, FT-IR, XRD, ^{13}C NMR and ^{15}N NMR. The non-isothermal reaction kinetics of the main exothermic decomposition reaction of HNTO was investigated by means of DSC. The thermodynamic properties of HNTO were calculated. The results showed that the formation of HNTO is achieved by proton transfer of N(4) atom, and it makes a higher nitrogen content and lower acidity. The reaction mechanism of HNTO is classified as nucleation and growth, and the mechanism function is Avramo–Erofeev equation with $n = 2/5$. The kinetic parameters of the reaction are $E_a = 195.29\,\text{kJ mol}^{-1}$, $\lg(A\ (\text{s}^{-1})) = 19.37$, respectively. The kinetic equation can be expressed as:

$$\frac{d\alpha}{dt} = 10^{18.97}(1-\alpha)[-\ln(1-\alpha)]^{3/5}\,e^{-2.35\times10^4/T}$$

The safety performances of HNTO were carried out. The critical temperature of thermal explosion are 464.26 and 474.37 K, the adiabatic time-to-explosion is 262 s, the impact sensitivity $H_{50} = 45.7$ cm, the friction sensitivity $P = 20\%$ and the electrostatic spark sensitivity $E_{50} > 5.4$ J (no ignition). It shows that HNTO has an insensitive nature as RDX and NTO, etc.

Keywords: Hydrazine 3-nitro-1,2,4-triazol-5-one complex (HNTO); Characterization; Non-isothermal reaction kinetics; Thermodynamic properties; Safety performances

1. Introduction

3-Nitro-1,2,4-triazol-5-one (NTO) is one of insensitive and high energetic materials, which has emerged as a new composite explosive with potential high safety performances, and is being explored as a substitute for hexogen (RDX) in munitions [1–4]. Owing to the acidic nature of NTO ($pK_a = 3.67$), it can form metal salts and amine salts with aromatic and aliphatic amines [5–8]. Hydrazine 3-nitro-1,2,4-triazol-5-one complex (HNTO) prepared by the reaction of NTO with hydrazine hydrate has an insensitive and high energetic nature as NTO and RDX materials. It has lower acidity than NTO, which makes it possess a higher chemical stability and consistency in propellant and explosive formulations, and a much preferable application range. It also has higher nitrogen content than NTO and RDX.

Studies on metal salts and amine salts of NTO have been reported in succession [1–11]. For HNTO, Lee claimed US patent right [7], but did not make further research, and there is little relative information in other literatures. In this paper, the

* Corresponding author. Fax: +86 29 88220423.
E-mail addresses: yiren@nwu.edu.cn, npecc@21cn.com (F.-q. Zhao).

0304-3894/$ – see front matter © 2007 Elsevier B.V. All rights reserved.
doi:10.1016/j.jhazmat.2007.08.064

preparation, characterization, non-isothermal reaction kinetics, thermodynamic properties and safety performances of HNTO were investigated.

2. Experimental

2.1. Synthesis

The title compound used in this research was prepared according to the following method: absolute ethanol solution of hydrazine hydrate was dropping into absolute ethanol solution of NTO (20% excess), kept stirring at 60 °C for 0.5–1.0 h. When the pH value came to 6.8–7.0, stopped the stirring. Then the product was filtrated, washed with deionized water and absolute ethanol in turn, and dried in vacuum oven at 80 °C, then the pure title compound was obtained. Some physical properties are appearance, yellow powder; purity, >99.90%; yield, 99.65%; real density, 1.82 g cm^{-3}.

2.2. Equipment and conditions

The contents of C, H, N and O elementals were determined on a Vario EL organic elemental analyzer (Elementar Co., Germany). The infrared spectra were recorded in the 4000–400 cm^{-1} region by using KBr pellets on a Nicolet 740 spectrometer (Nicolet Co., USA). X-ray diffraction (XRD) data were obtained by a D/MAX-2400 XRD analyzer (Rigaku Co., Japan), Cu target, Kα ray, wavelength λ = 1.5406 Å, scan rate 4° min^{-1}, step length 0.02°. ^{13}C NMR spectra and ^{15}N NMR spectra were obtained by a 500 MHz (Bruker Co., Germany) nuclear magnetic resonance (NMR) apparatus with dimethyl sulphoxide (DMSO) as solvent and internal standard material.

DSC curves were obtained by a TA 910S differential scanning calorimeter (TA Co., USA) under the condition of flowing nitrogen gas (purity, 99.999%; flowing rate, 60 cm^3 min^{-1}; atmospheric pressure). The conditions of DSC were sample mass, about 0.5 mg; heating rates (β), 2.5, 5, 7.5 and 10 K min^{-1}; reference sample, α-Al_2O_3. The DSC was calibrated with metals of In and Pb. Heating rate is calculated according to the actual rate of temperature rise from room temperature to the temperature at the end of decomposition.

The specific heat capacity (C_p, J mol^{-1} K^{-1}) of HNTO was determined with continuous C_p mode on a Micro-DSC III mircocalorimeter (Setaram Co., France). Heating rate, 0.15 K min^{-1}; sample mass, 101.52 mg; atmosphere, nitrogen. The mircocalorimeter was calibrated with α-Al_2O_3 (calcined), its math expression was C_p (J g^{-1} K^{-1}) = 0.1839 + 1.9966 × 10^{-3}T (283 K < T < 353 K), and the standard specific heat capacity $C^{\theta}_{p,m}(\alpha - Al_2O_3)$ at 298.15 K was determined as 79.44 J mol^{-1} K^{-1}.

The sensitivities of the title compound and original material NTO to impact stimuli were determined by a WL fall hammer apparatus containing a 5 kg drop weight with the standard Bruceton staircase method. Sample mass is 50 mg. The height for 50% probability of explosion (H_{50}, cm) was determined statistically.

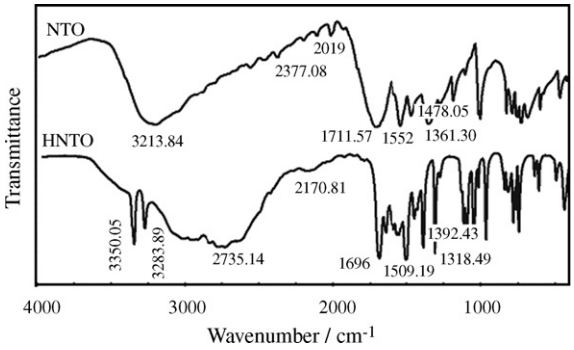

Fig. 1. FT-IR spectra of NTO and HNTO.

The friction sensitivities were determined on a WM-1 pendulum friction apparatus containing a 1.5 kg pendulum hammer fixed on 90° tilt angle. Gauge pressure is 3.92 MPa, sample mass is 20 mg. The probability of explosion (P, %) was determined statistically [12]. The spark sensitivities (E_{50}, J) were determined on a JGY-50 sensitivity instrument (No. 213 Research Institute of CNGC, China) [13].

3. Results and discussion

3.1. Characterization

Elemental anal. (%) calcd. for $C_2N_6H_6O_3$: C 14.81, H 3.70, N 51.83, O 29.62; found: C 15.02, H 3.75, N 51.51, O 29.33. The experimentally determined values are in close agreement with the theoretical ones corresponding to the general formula of $C_2N_4H_1O_3^-{\cdot}^+H_3NNH_2$ for HNTO. There is not crystal water in molecules. Molecular mass is 162.11.

The difference of FT-IR spectra (ν, cm^{-1}) of HNTO and NTO could be found in Fig. 1. The formation of HNTO prepared by the reaction of NTO with hydrazine hydrate was confirmed by the appearance of new strong and acuate IR bands at 3350.05 and 3283.89 due to –NH of hydrazine group, and the red shift of the other characteristic absorption bands: –NH in triazole ring shifts from 3213.84 to 2735.14; >C=O, from 1711.57 to 1696; ≡C–NO_2, from 1552, 1361.30 to 1509.19, 1318.49, respectively. The red shift indicated that the reaction of hydrazine hydrate with NTO induces the electron cloud density of carbonyl and nitryl to decline. The scheme of HNTO is shown in Fig. 2.

The XRD patterns of NTO and HNTO are shown in Figs. 3 and 4, the locations of strong rays (2θ, °) and relative intensity ($I \cdot I^{-1}$, %) are listed in Table 1. From Table 1, 2θ

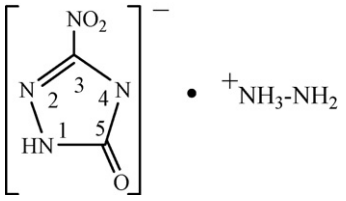

Fig. 2. Scheme of HNTO.

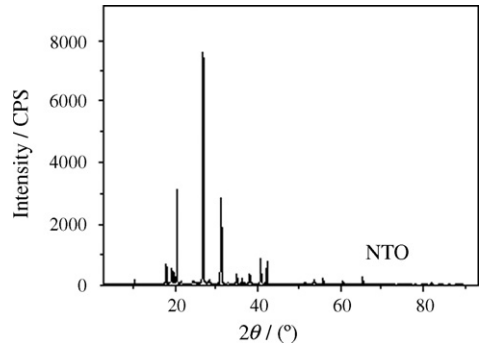

Fig. 3. XRD patterns of NTO.

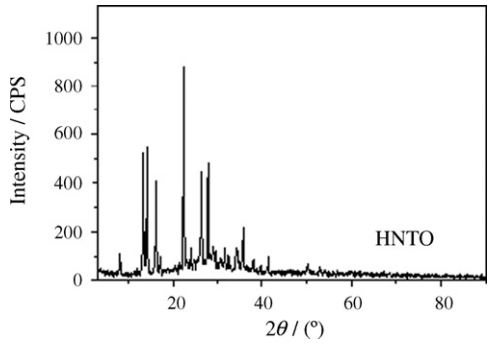

Fig. 4. XRD patterns of HNTO.

and $I \cdot I^{-1}$ of NTO and HNTO are quite different which means HNTO is a new product derived from NTO.

For HNTO, all of hydrogen atoms are combined with nitrogen atoms, and the strong activity makes it disadvantaged to analyze the structure and difficult to provide accurate data from ^{1}H NMR spectra. But there are only two isolated carbon atoms located in HNTO parent molecules, and the chemical shifts (δ) of the two carbon atoms can be used to approve the generation of the new compound. Comparing with the ^{13}C NMR spectrum of NTO in Fig. 5, the ^{13}C NMR spectrum of HNTO in Fig. 6 indicates two down-field chemical shift to 164.6 and 159.3 ppm of the carbon-atoms attached to the carbonyl group and nitro group, respectively, which demonstrates that the electron cloud density of NTO ring declines after HNTO complex formed, and the effect on the two carbon atoms is identical approximately.

Table 1
XRD data of NTO and HNTO

Compound	2θ (°)	$I \cdot I^{-1}$ (%)
NTO	20.76	36
	27.04	100
	31.34	36
HNTO	13.30	60
	14.20	58
	16.24	45
	22.38	100
	26.30	48
	27.72	48
	35.62	21

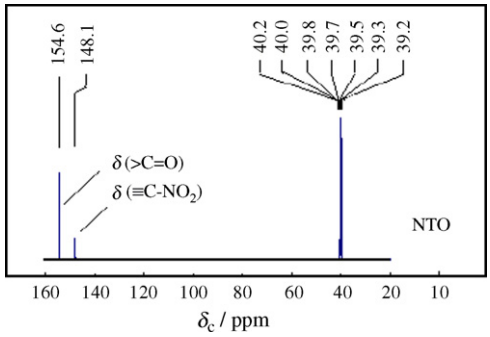

Fig. 5. ^{13}C NMR spectrum of NTO (DMSO-d_6, 25 °C).

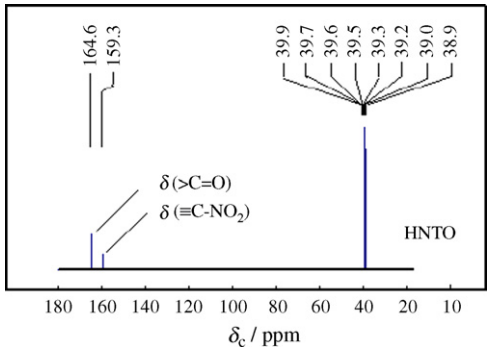

Fig. 6. ^{13}C NMR spectrum of HNTO (DMSO-d_6, 25 °C).

Comparing with the ^{15}N NMR spectrum of NTO in Fig. 7, Fig. 8 shows the ^{15}N NMR spectrum of HNTO composed of five different signals. The signals at 361.1, 268.2, 192.8, 182.7 and 49.3 ppm are attributed to –NO_2 group, N(2) group, N(1) group, N(4) group, and –NH_2 group, respectively, which demonstrates that nitrogen atoms in HNTO ring are all affected by hydrazine, and the effects rely on the position located in the ring to a great extent.

Therefore, it can be concluded that the formation of HNTO is achieved by the proton transfer of N(4) atom in NTO ring to hydrazine.

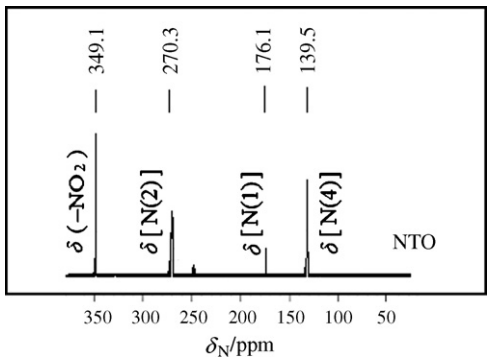

Fig. 7. ^{15}N NMR spectrum of NTO (DMSO-d_6, 25 °C).

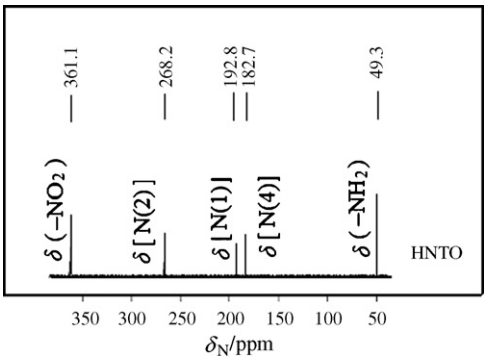

Fig. 8. ^{15}N NMR spectrum of HNTO (DMSO-d_6, 25 °C).

3.2. Non-isothermal reaction kinetics calculation [2–4,14,15]

In order to explore the thermal decomposition mechanism of the main exothermic reaction stage of HNTO and obtain the corresponding kinetic parameters (apparent activation energy (E_a), pre-exponential constant (A)) and the most probable kinetic model function, the DSC curves at heating rates of 2.5, 5, 7.5 and 10 K min^{-1} (the DSC curve at 10 K min^{-1} is shown in Fig. 9) were dealt by mathematic means, five integral methods (Eqs. (1)–(5)) and one differential method (Eq. (6)) listed in Table 2 are employed.

In these equations, α is the conversion degree, T is the temperature (K), T_p, the peak temperature in the DSC curve; R is the gas constant, $f(\alpha)$ and $G(\alpha)$ are the differential model function and the integral model function, respectively, E_a, A and β are mentioned above. The data needed for the equations of the integral and differential methods, i, α_i, β, T_i, T_e (onset temperature)

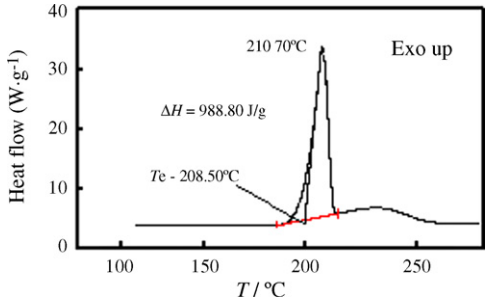

Fig. 9. DSC curve of HNTO (β = 10 K min^{-1}).

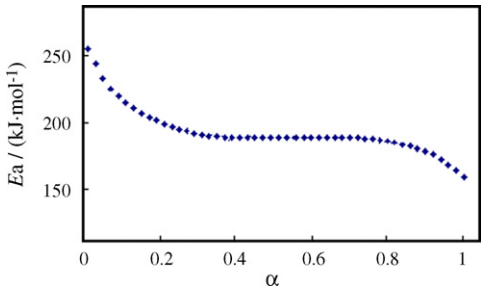

Fig. 10. The E_a–α curve obtained by Ozawa's method.

and T_p are obtained from the DSC curves and summarized in Table 3.

The values of E_a were obtained by Ozawa's method (Eq. (5)) with α changing from 0.01 to 1.00 and the E_a–α curve is shown in Fig. 10. From Fig. 10 we can find that activation energy making great changes with the increase of conversion degree except for the section of 0.25–0.85 (α). In this section, activation energy changes faintly, which means that the decomposition mechanism of the process does not transferred in essence or the transference could be ignored. So, it is feasible to study the reaction mechanism and kinetics in this section.

Forty-one types of kinetic model functions in Ref. [14] and the original data (data points 25–85) tabulated in Table 3 are put into Eqs. (1)–(6) for calculation, respectively. The values of E_a, lg(A (s^{-1})), linear correlation coefficient (r) and standard mean square deviation (Q) calculated on computer with the linear least-squares method at various heating rates of 2.5, 5, 7.5 and 10 K min^{-1} are listed in Table 4. The most probable mechanism function was selected by the better values of r, and Q based on the following four conditions: (1) the values of E_a (kJ mol^{-1}) and lg(A (s^{-1})) selected are in the ordinary range of the thermal decomposition kinetic parameters for solid materials (E_a (kJ mol^{-1}) = 80–250 and lg(A (s^{-1})) = 7–30); (2) linear correlation coefficient (r) is greater than 0.98; (3) the values of E_a (kJ mol^{-1}) and lg(A (s^{-1})) obtained with the differential and integral methods are approximately the same; (4) the mechanism function selected must be in agreement with the tested sample state. The results of satisfying the above-mentioned conditions at the same time are the final results as listed in Table 4.

The values of E_a (kJ mol^{-1}) and lg(A (s^{-1})) obtained from a single non-isothermal DSC curve are in good agreement approximately with the values calculated by Kissinger's

Table 2
Kinetic analysis methods

Method	Equation	
Ordinary-integral	$\ln[G(\alpha)/T^2] = \ln[(AR/\beta E)(1-2RT/E)] - E/RT$	(1)
Mac Callum–Tanner	$\lg[G(\alpha)] = \lg(AE/\beta R) - 0.4828E^{0.4357} - (0.449+0.217E)/0.001T \quad (E \text{ (kcal mol}^{-1}))$	(2)
Šatava–Šesták	$\lg[G(\alpha)] = \lg(A_S E_S/\beta R) - 2.315 - 0.4567E_S/RT$	(3)
Agrawal	$\ln[G(\alpha)/T^2] = \ln\left\{(AR/\beta E)[1-2(RT/E)]/[1-5(RT/E)^2]\right\} - E/RT$	(4)
Flynn–Wall–Ozawa	$\lg\beta = \lg\{AE/[RG(\alpha)]\} - 2.315 - 0.4567E/RT$	(5)
Kissinger	$\ln(\beta_i/T_{pi}^2) = \ln(A_k R/E_k) - E_k/RT_{pi}, \quad i = 1, 2, \ldots, 4$	(6)

Table 3
Data for the decomposition process of HNTO determined by DSC at different heating rates

Data point	α	T/K				Data point	α	T/K			
		$\beta = 2.5\ \mathrm{K\ min^{-1}}$	$\beta = 5\ \mathrm{K\ min^{-1}}$	$\beta = 7.5\ \mathrm{K\ min^{-1}}$	$\beta = 10\ \mathrm{K\ min^{-1}}$			$\beta = 2.5\ \mathrm{K\ min^{-1}}$	$\beta = 5\ \mathrm{K\ min^{-1}}$	$\beta = 7.5\ \mathrm{K\ min^{-1}}$	β=10 $\mathrm{K\ min^{-1}}$
1	0.01	457.44	458.55	463.12	465.25	51	0.51	469.29	474.71	479.23	482.38
2	0.02	458.52	460.38	464.76	467.03	52	0.52	469.38	474.82	479.34	482.49
3	0.03	459.29	461.58	465.90	468.27	53	0.53	469.47	474.93	479.45	482.60
4	0.04	459.90	462.50	466.81	469.25	54	0.54	469.57	475.03	479.56	482.71
5	0.05	460.43	463.27	467.58	470.08	55	0.55	469.66	475.14	479.67	482.81
6	0.06	460.89	463.93	468.26	470.80	56	0.56	469.74	475.23	479.77	482.91
7	0.07	461.31	464.52	468.87	471.45	57	0.57	469.83	475.33	479.87	483.01
8	0.08	461.69	465.05	469.43	472.03	58	0.58	469.92	475.43	479.97	483.11
9	0.09	462.05	465.54	469.94	472.58	59	0.59	470.00	475.52	480.07	483.20
10	0.10	462.38	465.99	470.41	473.08	60	0.60	470.08	475.62	480.17	483.29
11	0.11	462.69	466.41	470.85	473.55	61	0.61	470.16	475.70	480.26	483.38
12	0.12	462.99	466.81	471.27	473.99	62	0.62	470.24	475.79	480.35	483.47
13	0.13	463.27	467.18	471.66	474.41	63	0.63	470.32	475.88	480.44	483.56
14	0.14	463.54	467.53	472.03	474.80	64	0.64	470.39	475.96	480.53	483.64
15	0.15	463.80	467.87	472.39	475.18	65	0.65	470.47	476.05	480.62	483.72
16	0.16	464.04	468.19	472.72	475.54	66	0.66	470.54	476.13	480.71	483.81
17	0.17	464.28	468.50	473.04	475.88	67	0.67	470.62	476.21	480.79	483.89
18	0.18	464.51	468.80	473.35	476.20	68	0.68	470.69	476.29	480.88	483.97
19	0.19	464.72	469.08	473.64	476.51	69	0.69	470.76	476.37	480.96	484.06
20	0.20	464.94	469.35	473.92	476.81	70	0.70	470.83	476.45	481.05	484.14
21	0.21	465.14	469.62	474.19	477.10	71	0.71	470.91	476.53	481.14	484.22
22	0.22	465.34	469.87	474.45	477.37	72	0.72	470.98	476.61	481.23	484.31
23	0.23	465.53	470.11	474.70	477.63	73	0.73	471.05	476.69	481.32	484.40
24	0.24	465.72	470.35	474.94	477.89	74	0.74	471.12	476.78	481.41	484.49
25	0.25	465.90	470.57	475.17	478.13	75	0.75	471.19	476.86	481.50	484.58
26	0.26	466.07	470.79	475.39	478.37	76	0.76	471.26	476.94	481.60	484.68
27	0.27	466.24	471.00	475.61	478.60	77	0.77	471.33	477.03	481.70	484.78
28	0.28	466.41	471.21	475.81	478.82	78	0.78	471.40	477.12	481.80	484.88
29	0.29	466.57	471.41	476.01	479.04	79	0.79	471.48	477.21	481.91	484.99
30	0.30	466.73	471.60	476.21	479.24	80	0.80	471.55	477.31	482.02	485.11
31	0.31	466.88	471.79	476.40	479.44	81	0.81	471.63	477.41	482.14	485.22
32	0.32	467.03	471.98	476.58	479.63	82	0.82	471.71	477.51	482.27	485.35
33	0.33	467.17	472.16	476.75	479.82	83	0.83	471.79	477.62	482.40	485.48
34	0.34	467.32	472.33	476.92	480.00	84	0.84	471.88	477.74	482.54	485.62
35	0.35	467.45	472.50	477.09	480.17	85	0.85	471.97	477.86	482.69	485.76
36	0.36	467.59	472.67	477.25	480.34	86	0.86	472.06	478.00	482.85	485.92
37	0.37	467.72	472.83	477.41	480.50	87	0.87	472.16	478.13	483.01	486.09
38	0.38	467.85	472.99	477.56	480.66	88	0.88	472.27	478.28	483.20	486.26
39	0.39	467.97	473.14	477.71	480.81	89	0.89	472.38	478.45	483.40	486.46
40	0.40	468.10	473.29	477.85	480.96	90	0.90	472.51	478.62	483.61	486.67
41	0.41	468.22	473.44	477.99	481.11	91	0.91	472.64	478.81	483.85	486.90
42	0.42	468.33	473.58	478.12	481.25	92	0.92	472.80	479.02	484.12	487.16
43	0.43	468.45	473.72	478.26	481.39	93	0.93	472.97	479.25	484.41	487.45
44	0.44	468.56	473.86	478.39	481.52	94	0.94	473.16	479.51	484.76	487.78
45	0.45	468.67	473.99	478.52	481.65	95	0.95	473.39	479.81	485.17	488.18
46	0.46	468.78	474.12	478.64	481.78	96	0.96	473.66	480.16	485.65	488.67
47	0.47	468.89	474.24	478.76	481.91	97	0.97	474.02	480.56	486.20	489.24
48	0.48	468.99	474.36	478.88	482.03	98	0.98	474.48	481.03	486.79	489.90
49	0.49	469.09	474.48	479.00	482.15	99	0.99	475.05	481.56	487.38	490.59
50	0.50	469.19	474.60	479.12	482.26	100	1.00	475.65	482.10	487.97	491.28
								464.05(T_e)	472.25(T_e)	476.85(T_e)	481.65(T_e)
								471.25(T_p)	476.45(T_p)	480.85(T_p)	483.85(T_p)

method and Ozawa's method. Therefore, conclusion could be drawn as that the reaction mechanism of the main exothermal decomposition process of HNTO is classified as nucleation and growth, and the mechanism function is Avramo–Erofeev equation with $n = 2/5$, $G(\alpha) = [-\ln(1-\alpha)]^{2/5}$, and $f(\alpha) = (2/5)(1-\alpha)[-\ln(1-\alpha)]^{3/5}$. Substituting $f(\alpha)$ with $(2/5)(1-\alpha)[-\ln(1-\alpha)]^{3/5}$, E_a (kJ $\mathrm{mol^{-1}}$) with 195.29 and lg(A ($\mathrm{s^{-1}}$)) with 19.37 into Eq. (7):

$$\frac{\mathrm{d}\alpha}{\mathrm{d}t} = A f(\alpha)\, \mathrm{e}^{-E/RT} \tag{7}$$

Table 4
Kinetic parameters obtained for the decomposition process of HNTO

Method	β/(K min^{-1})	E_a (kJ mol^{-1})	lg(A (s^{-1}))	r	Q
Ordinary-integral	2.5	217.90	21.92	0.9955	0.0225
	5	187.34	18.51	0.9939	0.0303
	7.5	188.34	18.59	0.9968	0.0162
	10	188.95	18.64	0.9950	0.0251
Mac Callum–Tanner	2.5	218.65	21.98	0.9958	0.0043
	5	187.97	18.54	0.9944	0.0057
	7.5	189.05	18.63	0.9970	0.0031
	10	189.71	18.69	0.9954	0.0047
Šatava–Šesták	2.5	214.63	21.60	0.9958	0.0043
	5	185.65	18.32	0.9944	0.5723
	7.5	186.67	18.41	0.9970	0.0031
	10	187.30	18.46	0.9954	0.0047
Agrawal	2.5	217.90	21.92	0.9955	0.2254
	5	187.34	18.51	0.9939	0.0303
	7.5	188.34	18.59	0.9968	0.0162
	10	188.95	18.64	0.9950	0.0251
Mean		195.29	19.37		
Flynn–Wall–Ozawa		196.74		0.9962	0.0016
Kissinger		198.95	19.72	0.9958	0.0083

and the kinetic equation of exothermal decomposition reaction may be described as:

$$\frac{d\alpha}{dt} = 10^{18.97}(1-\alpha)[-\ln(1-\alpha)]^{3/5}\, e^{-2.35\times10^4/T}$$

3.3. Determination of thermodynamic properties

3.3.1. Specific heat capacity

The determination and simulations results of specific heat capacity of HNTO are shown in Fig. 11.

In the figure, $C_{p,1}$ and $C_{p,2}$ are linear and parabolic simulation respectively of specific heat capacity of HNTO:

$$C_{p,1}(J\,g^{-1}\,K^{-1}) = 2.14\times10^{-1} + 3.20\times10^{-3}T \quad (283.4\,K < T < 344.7\,K) \tag{8}$$

$$C_{p,1}(J\,mol^{-1}\,K^{-1}) = 34.69 + 0.52T \quad (283.4\,K < T < 344.7\,K) \tag{9}$$

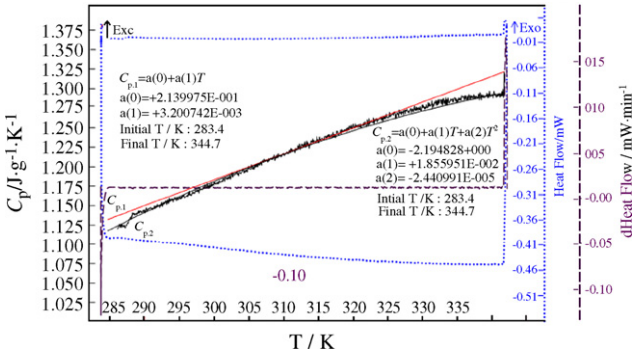

Fig. 11. Determination curve of the continuous specific heat capacity of HNTO.

$$C_{p,2}(J\,g^{-1}\,K^{-1}) = -2.19 + 1.86\times10^{-2}T - 2.44\times10^{-5}T^2 \quad (283.4\,K < T < 344.7\,K) \tag{10}$$

$$C_{p,2}(J\,mol^{-1}\,K^{-1}) = -355.02 + 3.02T - 3.96\times10^{-3}T^2 \quad (283.4\,K < T < 344.7\,K) \tag{11}$$

The values of specific heat capacity at 298.15 K are $C_{p,1}$ (298.15 K) = 189.36 J mol^{-1}; $C_{p,2}$ (298.15 K) = 192.36 J mol^{-1}, respectively. From Fig. 11, we can find that the C_p value calculated with the parabolic expression is much closer to the measured one than that of the linear expression as the temperature range extrapolating outside the temperature range of 283.4–344.7 K. And $C_{p,2}$ is preferred.

3.3.2. Thermodynamic functions

The enthalpy change, entropy change and Gibbs free energy change of HNTO were calculated by Eqs. (12)–(14) at 283–353 K taking 298.15 K as the benchmark. The results are listed in Table 5.

$$H_r - H_{298.15} = \int_{298.15}^{T} C_p\,dT \tag{12}$$

$$S_r - S_{298.15} = \int_{298.15}^{T} C_p T^{-1}\,dT \tag{13}$$

$$G_r - G_{298.15} = \int_{298.15}^{T} C_p\,dT - T\int_{298.15}^{T} C_p T^{-1}\,dT \tag{14}$$

where $C_p = C_{p,2}$ as Eq. (11) expressed.

Table 5
Thermodynamic functions of HNTO

T (K)	$(H_r-H_{298.15})$ (kJ mol^{-1})	$(S_r-S_{298.15})$ (J mol^{-1} k^{-1})	$(G_r-G_{298.15})$ (kJ mol^{-1})
283.0	−2.8382	−9.7760	−0.0716
293.0	−0.9776	−3.3112	−0.0074
303.0	0.9356	3.1273	−0.0120
313.0	2.9433	9.5921	−0.0590
323.0	4.9669	16.0306	−0.2110
333.0	7.0692	22.4428	−0.4042
343.0	9.1979	289.0762	−89.9553
353.0	11.3791	341.6355	−109.2182

3.3.3. $\Delta S^{\neq}$, $\Delta H^{\neq}$ and $\Delta G^{\neq}$

The entropy of activation ($\Delta S^{\neq}$), enthalpy of activation ($\Delta H^{\neq}$), and free energy of activation ($\Delta G^{\neq}$) obtained by Eqs. (15)–(17) [14,15] are 231.03 J mol^{-1} K^{-1}, 195.09 kJ mol^{-1} and 87.71 kJ mol^{-1}, respectively.

$$A = \frac{k_B T}{h} e^{\Delta S^{\neq}/R} \tag{15}$$

$$\Delta H^{\neq} = E_a - RT \tag{16}$$

$$\Delta G^{\neq} = \Delta H^{\neq} - T\,\Delta S^{\neq} \tag{17}$$

where $T = T_{p0}$, obtained by Eq. (18) (see the Section 3.4.1), 464.80 K; $E_a = E_k$, the value of E_a calculated by Kissinger's method, 198.95 kJ mol^{-1}; $A = A_k$, the value of A calculated by Kissinger's method, $10^{19.72}$ s^{-1}; k_B, Boltzmann constant, 1.3807×10^{-23} J K^{-1}; h, Plank constant, 6.626×10^{-34} J s^{-1}.

3.4. Safety performances assessing

3.4.1. Calculation of critical temperatures of thermal explosion

The values (T_{eo} and T_{po}) of the onset temperature (T_e) and peak temperature (T_p) corresponding to $\beta \to 0$ obtained by Eq. (18) taken from [15,16] are 455.10 and 464.80 K, respectively.

$$T_{(e\,or\,p)_i} = T_{eo\,or\,op} + b\beta_i + c\beta_i^2, \quad i = 1\text{–}4 \tag{18}$$

where b and c are coefficients.

The corresponding critical temperatures of thermal explosion (T_{be} and T_{bp}) obtained from Eq. (19) taken from Refs. [15,16] are 464.26 and 474.37 K, respectively. The T_{bp} value is close to that of RDX (482.15 K) and lower than that of NTO (539.15 K).

$$T_{be\,or\,bp} = \frac{E_O - \sqrt{E_O^2 - 4E_O R T_{eo\,or\,po}}}{2R} \tag{19}$$

where R is the gas constant (8.314 J mol^{-1} K^{-1}) and E_O is the value of E_a calculated by Ozawa's method.

3.4.2. Estimation of the adiabatic time-to-explosion

The adiabatic time-to-explosion (t, s) of energetic materials is the time of energetic material thermal decomposition transiting to explosion under the adiabatic conditions, and is an important parameter for assessing the thermal stability and the safety of energetic materials. The estimation formula of adiabatic time-to-explosion of energetic materials is showed as Eq. (20) taken from [17,18], and t value obtained by the definite integral equation is 262 s.

$$C_p \frac{dT}{dt} = QA \exp\left(\frac{-E}{RT}\right) f(\alpha)$$

$$\Rightarrow \quad t = \frac{1}{QA} \int_{T_0}^{T} \frac{C_p \exp(E/RT)}{f(\alpha)}\, dT \tag{20}$$

where $C_p = C_{p,2}$ as Eq. (11) expressed, and the temperature range extrapolating from 283.4–344.7 to 455.10–474.37 K; $f(\alpha)$, differential mechanism function $(2/5)(1-\alpha)[-\ln(1-\alpha)]^{3/5}$; E, activation energy, 195.29 kJ mol^{-1}; A, pre-exponential constant, $10^{19.37}$ s^{-1}; Q, decomposition heat, 160.29 kJ mol^{-1}; n, decomposition reaction order, 2/5; R, the gas constant, 8.314 J mol^{-1} K^{-1}; α, the conversion degree, and

$$\alpha = \int_{T_0}^{T} \frac{C_p}{Q}\, dT \tag{21}$$

where the integral upper limit $T = T_{bp} = 474.37$ K and the lower limit $T_0 = T_{eo} = 455.10$ K.

In the calculation process of adiabatic time-to-explosion, a little change in the activation energy located in the integral equation with exponential form can make a great difference in the result, and a small increase of the activation energy can induces adiabatic time-to-explosion to rise greatly.

3.4.3. Mechanical and electrostatic spark sensitivities

The mechanical and electrostatic spark sensitivities were determined according to the method of literature [12,13,19] and listed in Table 6.

From Table 6, we can find that HNTO is less insensitive than NTO and more insensitive than RDX for mechanical sensitivities, and it has an excellent electrostatic spark sensitivity. In general, HNTO has an insensitive nature comparing with RDX and NTO.

Table 6
The mechanical and electrostatic spark sensitivity of HNTO comparing with NTO and RDX

Test	HNTO	NTO	RDX
Impact sensitivity H_{50} (cm)	45.7	77	22
Friction sensitivity P (%)	20	4	76
Electrostatic spark sensitivity E_{50} (J)	>5.4 (No ignition)	>4.5 (No ignition)	4.5 (Ignition)

4. Conclusions

Hydrazine 3-nitro-1,2,4-triazol-5-one complex (HNTO) was prepared by the reaction of 3-nitro-1,2,4-triazol-5-one with hydrazine hydrate. The formation of HNTO is achieved by proton transfer of N(4) atom. The main exothermic decomposition reaction mechanism of HNTO is classified as nucleation and growth, and the mechanism function is Avramo–Erofeev equation with $n = 2/5$. The kinetic parameters of the reaction are $E_a = 195.29\ \mathrm{kJ\ mol^{-1}}$, $\lg(A\ (\mathrm{s^{-1}})) = 19.37$, respectively. The kinetic equation can be expressed as:

$$\frac{d\alpha}{dt} = 10^{18.97}(1-\alpha)[-\ln(1-\alpha)]^{3/5}\, e^{-2.35\times10^4/T}.$$

The critical temperature of thermal explosion (T_{bp}) of HNTO is close to that of RDX and lower than that of NTO. The adiabatic time-to-explosion is 262 s. It also has a good mechanical and electrostatic spark sensitivity comparing with RDX and NTO.

Acknowledgements

Project supported by the National Natural Science Foundation of China (No. 20573098) and the Foundation of Key Laboratory of Science and Technology for National Defence of Propellant and Explosive of China (No. 9140C3503020605).

References

[1] K.Y. Lee, L.B. Chapman, M.D. Coburn, A less sensitive explosive: 3-nitro-1,2,4-triazol-5-one, J. Ener. Mater. 5 (1) (1987) 27–33.
[2] T.L. Zhang, Study on Preparation, Structure Characterization, Decomposition Mechanism and Non-isothermal Reaction Kinetics of NTO, East China University of Science & Technology, Shanghai, 1993 (in Chinese).
[3] J.R. Song, Study on NTO Metal Complex, first ed., Chemical Industry Press, Beijing, 1998 (in Chinese).
[4] H.X. Ma, J.R. Song, R.Z. Hu, Non-isothermal kinetics of the thermal decomposition of 3-nitro-1,2,4-triazol-5-one magnesium complex, Chin. J. Chem. 21 (12) (2003) 1558–1561.
[5] J.R. Li, B.R. Chen, Y.X. Ou, G.Y. Fan, X.S. Cui, The crystal structure of lead 3-nitro-1,2,4-triazol-5-one (NTO), J. Beijing Inst. Technol. 13 (1993) 157–160.
[6] C.G. Feng, L. Yang, J.G. Zhang, Preparation and molecular structure of CHZNTO·H_2O, Chin. J. Struct. Chem. 21 (3) (2002) 309–312.
[7] K.Y. Lee, M.D. Coburn, 3-Nitro-1,2,4-triazol-5-one: A less sensitive explosive, USP 4,733,610, 1988.
[8] G. Singh, I.P.S. Kapoor, S. Mudi Mannan, S.K. Tiwari, Studies on energetic compounds, Part 7: kinetics of thermolysis of ring-substituted arylammonium salts of NTO, J. Energ. Mater. 16 (1998) 101.
[9] G. Singh, I.P.S. Kapoor, S.K. Tiwari, S.P. Felix, Studies on energetic compounds, Part 12: preparation and thermolysis of transition metal salts of 5-nitro-2,4-dihydro-3H-1,2,4-triazole-3-one (NTO), Indian J. Eng. Mater. Sci. 7 (2000) 167.
[10] G. Singh, I.P.S. Kapoor, S.K. Tiwari, S.P. Felix, K.N. Ninan, T.L. Varghese, Studies on energetic compounds, Part 15: transition metal salts of NTO as potential energetic burning rate catalysts for composite solid propellants, J. Energ. Mater. 20 (3) (2002) 309.
[11] G. Singh, S.P. Felix, Studies on energetic compounds 25: an overview of preparation, thermolysis and applications of the salts of 5-nitro-2,4-dihydro-3H-1,2,4-triazol-3-one (NTO), J. Hazard. Mater. A90 (2002) 1–17.
[12] Ammunition standard of PRC, Testing methods of sensitivity and safe property, GJB/772A-97.
[13] Ammunition standard of PRC, Testing methods of pyrotechnic device-Electrostatic sensitivity of electronic pyrotechnic devices, GJB736.11-90.
[14] R.Z. Hu, Q.Z. Shi, Thermal Analysis Kinetics, first ed., Science Press, Beijing, 2001 (in Chinese).
[15] R.Z. Hu, S.P. Chen, S.L. Gao, F.Q. Zhao, Y. Luo, H.X. Gao, Q.Z. Shi, H.A. Zhao, P. Yao, J. Li, Thermal decomposition kinetics of the $Pb_{0.25}Ba_{0.75}$(TNR)·H_2O complex, J. Hazard. Mater. A117 (2005) 103–110.
[16] T.L. Zhang, R.Z. Hu, Y. Xie, F.P. Li, The estimation of critical temperatures of thermal explosion for energetic materials using non-isothermal DSC, Thermochim. Acta 244 (1994) 171–176.
[17] L.C. Smith, An approximate solution of the adiabatic explosion problem, Thermochim. Acta 13 (1) (1975) 1–6.
[18] R.Z. Hu, H. Zhang, Z.M. Xia, P.J. Guo, S.L. Gao, Q.Z. Shi, G.E. Lu, J.Y. Jiang, Estimation formulae of the critical rate of temperature rise for thermal explosion of exothermic decomposition reaction system of energetic materials, Chin. J. Energ. Mater. 11 (3) (2003) 130–133, 137.
[19] S.Y. Xu, F.Q. Zhao, S.W. Li, H.X. Hao, Q. Pei, H.X. Gao, Impact and friction sensitivity of composite modified double base propellant containing hexanitrohexaazaisowurtzitane (CL-20), 37th ICT, V08 (2006) 1–6.